Noise and Vibration: *Emerging Methods*
**NOVEM 2009**
5-8 April 2009 Oxford

# NEARFIELD STRUCTURE–BORNE SOUND HOLOGRAPHY

M. Cavallari[1*], H. A. Bonhoff[2] and B. A. T. Petersson[3]

[1]Dept. Of Engineering, University of Ferrara, Via Saragat 1, 44100, Ferrara
Email: marco.cavallari@unife.it

[2] Institute of Fluid Mechanics and Engineering Acoustics, Technische Universität Berlin,
Einsteinufer 25, 10587 Berlin
Email: hannes.bonhoff@tu-berlin.de

[3] Institute of Fluid Mechanics and Engineering Acoustics, Technische Universität Berlin,
Einsteinufer 25, 10587 Berlin
Email: b.a.t.petersson@tu-berlin.de

## ABSTRACT

*In conjunction with inverse problems, nearfield acoustical holography can be used to predict the pressure, the velocity components and the acoustic intensity vector generated by a source. The aim of the present work is at developing a theoretical platform for nearfield structure-borne sound holography, useful to predict velocity and forces acting on a plate, as well as the transmitted power of source-receiver installations. Numerical simulations are undertaken to investigate the practicability of the theory and to study the applicability for an infinite plate excited by a number of point forces. An experimental rig has been constructed, suitably designed to suppress the reflections from the boundaries. Using this approach, the velocities, the forces and the transmitted power are calculated. Experimental results are presented in order to validate the technique and some tests are reported to establish the limit of validity. Since the quantities calculated using nearfield structure-borne sound holography show the same trends as the quantities directly measured on the plate in a wide frequency range, the results must be considered promising.*

## 1 INTRODUCTION

In several practical cases one knows the exact position of the excitation points but it is impossible to directly measure the amplitude of the forces acting on the structure. This situation occurs for example when one cannot place transducers at the points of support of a machinery. As stated in [1], the knowledge of the dynamic force intensity acting on the structure is very important to determine the vibratory behaviour and to predict the possible effects of structural changes. In the majority of practical installations it is not possible to place a force transducer directly between the excitation source and the structure. In a more specific way, we can say that the knowledge of forces and velocities in correspondence with the excitation points is the first step to a proper structure-borne sound source characterization [2]. In this light, physical theories allow us to make predictions.

For example, after having described the physical system completely, it is possible to predict the response to an excitation. This is a simulation problem, or a forward problem:

$$F(x) \Rightarrow \begin{cases} u(x) \\ v(x) = \dot{u}(x) \\ a(x) = \ddot{u}(x) \end{cases} \tag{1}$$

On the other hand, the same theories that allow to make predictions by modelling the system with the a priori knowledge of some parameters, allow also to infer from the result of some measurements to the causes that determined it:

$$\left.\begin{array}{l} u(x) \\ v(x) = \dot{u}(x) \\ a(x) = \ddot{u}(x) \end{array}\right\} \Rightarrow F(x) \tag{2}$$

This is the typical example of a inverse problem [3] and the nearfield structure-borne sound holography is an application of this kind of problems.
An application of the inverse problem for the calculation of the force distribution on a beam can be found in [4]. The force field is reconstructed from the sampling of the displacement on the entire structure by discretizing the basic equation of motion of the system. In [5] this method is extended to plates, where the structure is discretized by a regular meshgrid on which measurements are carried out. In [6] and [7] a different approach based on the structural intensity is used. Once again the entire plate is discretized by a mesh to reconstruct the force field.
The present work deals with a different target: to predict velocity and forces acting on a plate, as well as the transmitted power of source-receiver installations without performing direct measurements in this area, but starting from measurements carried out close to the source. The idea is similar to the basic concept of nearfield acoustical holography, used to predict the pressure values, the velocity components and the intensity vector generated by a source [8]. In the case of nearfield structure-borne sound holography, the force and the velocity values can be computed, as well as the transmitted power, starting from measurements in the near field. In the present work the test case of an infinite Perspex plate excited by a laboratory source in four points will be examined to fix the practicability of this novel approach as well as the limit of the theory.

## 2 FUNDAMENTAL THEORY

As stated in the introduction, one of the goals of the present work is to determine velocities and forces at several excitation points on a Perspex plate, starting from velocity measurements along two external circular curves. The computation of waves that propagate inward would be problematic, so only the infinite plate case is studied first of all with a numerical simulation, then with an experimental validation.

### 2.1 Formulation of plate velocity

Since we are dealing with an infinite plate, we can use the velocity measurements on two external circular curves as a boundary condition for the equation of motion. By subsequently back-propagating the velocity, it is possible to determine the velocity on an internal circular line, which passes on the excitation points. The velocity along the external circle is called $v(r_2)$, the velocity along the internal circle is called $v(r_1)$, the velocity along the middle circle

is called $v(r_m)$, and finally $v(r_0)$ is the velocity on the interface circle. Using the geometry shown in Figure 1 one can apply the theory only to sources with feet lying on the same circular line, otherwise one must take into consideration also the waves propagating inward.

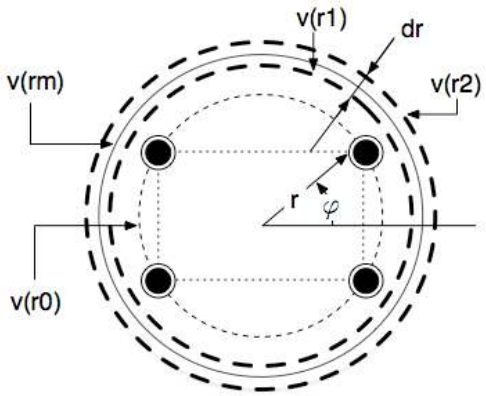


Figure 1: Geometry scheme.

With reference to Figure 1, $r_m$ is the average radius between $r_1$ and $r_2$. In this way, starting from the velocities measured on the two external circular lines it is possible to approximate the velocity on the circumference with radius $r_m$ by averaging $v(r_1)$ and $v(r_2)$. It is also possible to determine the rotational velocity $w(r_m)$ which equals the first derivative of the translational velocity with respect to the radius coordinate.

$$w(r_m) = \frac{\partial v(r)}{\partial r} \tag{3}$$

Since we are dealing with a discrete velocity measurement, we can discretize equation (3) in the form:

$$w(r_m) \cong \frac{v(r_2) - v(r_1)}{r_2 - r_1} \tag{4}$$

The velocities $v(r_m)$ and $w(r_m)$ have to be expanded in orders to apply the infinite plate equation of motion. For the velocities on the radius $r_m$, the generic orders can be obtained with the Fourier transform in the angular domain:

$$v_n(r_m) = \int_0^{2\pi} v(r_m, \varphi) e^{-jk_n\varphi} d\varphi \tag{5}$$

$$w_n(r_m) = \int_0^{2\pi} w(r_m, \varphi) e^{-jk_n\varphi} d\varphi \tag{6}$$

Accordingly with the theory, an infinite plate excited by a point force must have a cylindrical symmetric response, so we can express the $n^{th}$ order using the Hankel function of order n and second kind, and two constants, $A$ and $B$ (see equation (7)) [9]. Since we are dealing with four excitation points, we will superimpose the responses due to each force because the plate behaviour can be considered linear.
The general equation for the translational velocity orders of an infinite plate is given in equation (7).

$$v_n(r) = A_n H_n^{(2)}(k_b r) + B_n H_n^{(2)}(-jk_b r) \tag{7}$$

With equation (3) and (7), the expression for the rotational velocity is found to be given by equation (8):

$$w_n(r) = A_n \frac{d}{dr} H_n^{(2)}(k_b r) + B_n \frac{d}{dr} H_n^{(2)}(-jk_b r) \tag{8}$$

Where $k_b$ is the wave number, which is a function of frequency and material properties.
If we measure the velocities $v(r_1)$ and $v(r_2)$, it is possible to determine $v(r_m)$ by an average and $w(r_m)$ using equation (4). Once $v(r_m)$ and $w(r_m)$ are determined, it is possible to calculate the constants $A$ and $B$ for each order.

$$A_n = \frac{1}{H_n^{(2)}(k_b r_m)} \left( v_n(r_m) + \frac{w_n(r_m) H_n^{(2)}(k_b r_m) - v_n(r_m) \frac{d}{dr}\left[ H_n^{(2)}(k_b r_m) \right]}{\frac{d}{dr}\left[ H_n^{(2)}(k_b r_m) \right] - \frac{H_n^{(2)}(k_b r_m)}{H_n^{(2)}(-jk_b r_m)} \frac{d}{dr}\left[ H_n^{(2)}(-jk_b r_m) \right]} \right) \tag{9}$$

$$B_n = \frac{w_n(r_m) H_n^{(2)}(k_b r_m) - v_n(r_m) \frac{d}{dr}\left[ H_n^{(2)}(k_b r_m) \right]}{H_n^{(2)}(k_b r_m) \frac{d}{dr}\left[ H_n^{(2)}(-jk_b r_m) \right] - H_n^{(2)}(-jk_b r_m) \frac{d}{dr}\left[ H_n^{(2)}(k_b r_m) \right]} \tag{10}$$

The n$^{th}$ order of the velocity along the interface circle (at radius $r_0$) can easily be determined using equation (7) once $A$ and $B$ are calculated. Finally the velocity along the interface circle is obtained by summing the orders for each angular position.

$$v(r_0, \varphi) = \sum_n v_n(r_0) e^{jk_n \varphi} \tag{11}$$

## 2.2 Calculation and discretization of forces

Once the velocity along the interface circular line is calculated using equation (11), we still have to find an expression for calculating the forces to fully characterize the source-receiver coupling.

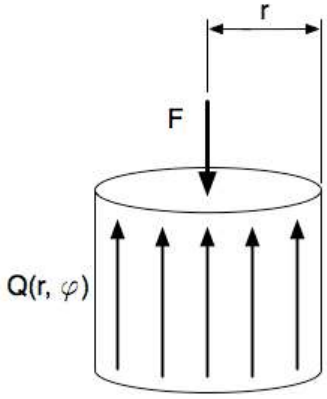


Figure 2: Force balance on a plate plug.

This relationship is provided by the plate–like structures' equation of motion: studying the force balance for a coordinate ($r$, $\varphi$), it is possible to write the following equation:

$$F = 2\pi r Q(r,\varphi) \tag{12}$$

Where $Q(r, \varphi)$ is the shear stress at radius $r$ and angular position $\varphi$.
In case of a single point excitation force, it can be expressed as:

$$Q(r,\varphi) = -B' k_b^2 \frac{\partial(k_b r)}{\partial r}\left[\frac{\partial H_0^{(2)}(k_b r)}{\partial k_b r} + \frac{\partial H_0^{(2)}(-jk_b r)}{\partial k_b r}\right] \tag{13}$$

Once we are dealing with a small plate plug, it is possible to use the expression of Hankel function for small arguments. In this way the expression for $Q(r, \varphi)$ becomes:

$$Q(r,\varphi) = \frac{4\,jB' k_b^2}{\pi r}\eta \tag{14}$$

Where $\eta$ is the displacement of the plug along the interface circle line. It can be calculated integrating the back–propagated velocity ($v(r_0)$) with respect to time. Finally, if we image to cut a plug around each point used to discretize the velocity, it is possible to express the forces acting on each plug of coordinate ($r_0$, $\varphi$) by integrating the shear force along the plug's contour:

$$F(r_0,\varphi) = 8\,jB' k_b^2 \eta \tag{15}$$

Equation (15) can be used to calculate the force value on the interface circumference.

### 2.3 Numerical evaluations

The theory described in the previous sections has been evaluated by a numerical simulation. First of all, the trace of the velocity along the interface circumference is investigated for various frequencies, not only to validate the results for the amplitude, but also to compare the shape of the plot of the back–calculated velocity and of the measured velocity at radius $r_0$. To do this comparison, the velocity field has been simulated on the plate. First of all we need to express the mobility for an infinite plate as reported in the following expression [10].

$$Y(r,\varphi) = Y^{\infty}\left[H_0^{(2)}(k_b r) - H_0^{(2)}(-jk_b r)\right] \tag{16}$$

The quantity $Y^{\infty}$ represents the infinite plate mobility. It can be calculated using equation (17).

$$Y^{\infty} = \frac{1}{8\sqrt{B'm''}} \tag{17}$$

In the equation above, $B'$ represents the bending stiffness of the plate and $m''$ the mass per unit of surface.
Once the mobility is known, it is possible to calculate the velocity for every point on the plate. Finally, we can apply the theory described in sections 2.1 and 2.2 in order to back–calculate

the velocity and the force. The equations and the two external circular lines have been discretized using 128 points. The velocity and the force have been expanded in 128 orders.
The results of the back-calculated velocity and force at 2 kHz are presented in Figure 3 and Figure 4.

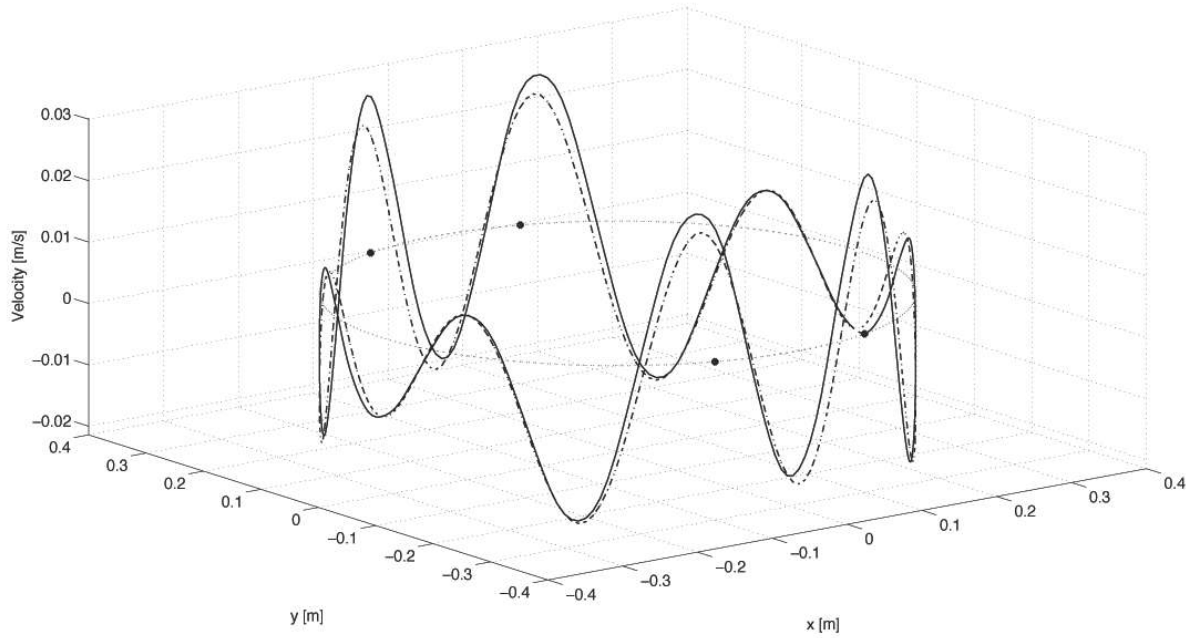


Figure 3: Comparison between imposed velocity (dash-dot line) and calculated velocity (solid line).

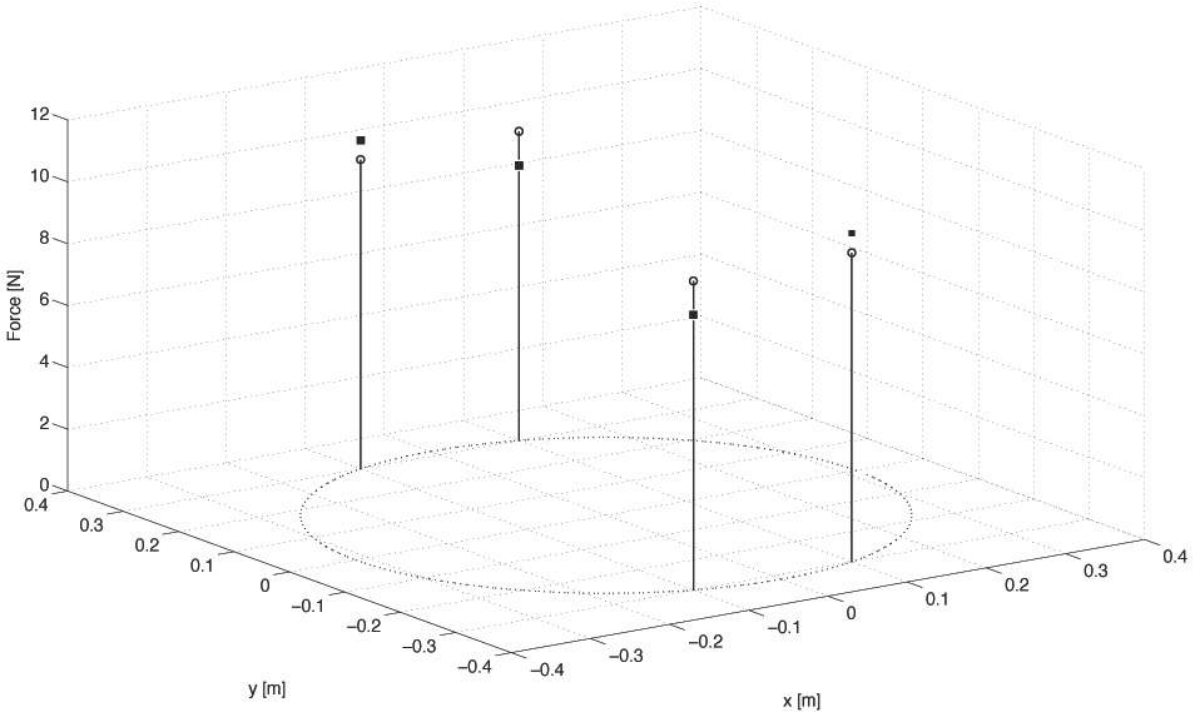


Figure 4: Comparison between imposed forces (circular marker) and calculated forces (square marker).

Since the results are promising both from the point of view of the shape and of the peaks' amplitude, the application of the formerly described theory can be extended also to an experimental test case.

## 3. EXPERIMENTAL ANALYSIS

After having validated the theory using a numerical simulation, the reliability of an application to measured data was checked. First of all an experimental rig was constructed, suitably designed to suppress the reflections from the boundaries. A Perspex plate suspended on a foam frame, with the edges embedded in sand can be considered as an infinite plate under certain assumptions (see section 3.1). The plate was excited in four points lying on the same circumference. To do this a source was built with a shaker mounted on a cylindrical frame with four feet. A force transducer and an accelerometer were fixed corresponding to each foot to validate the inverse problem results. The coupling between the plate and the source is reported in Figure 5.

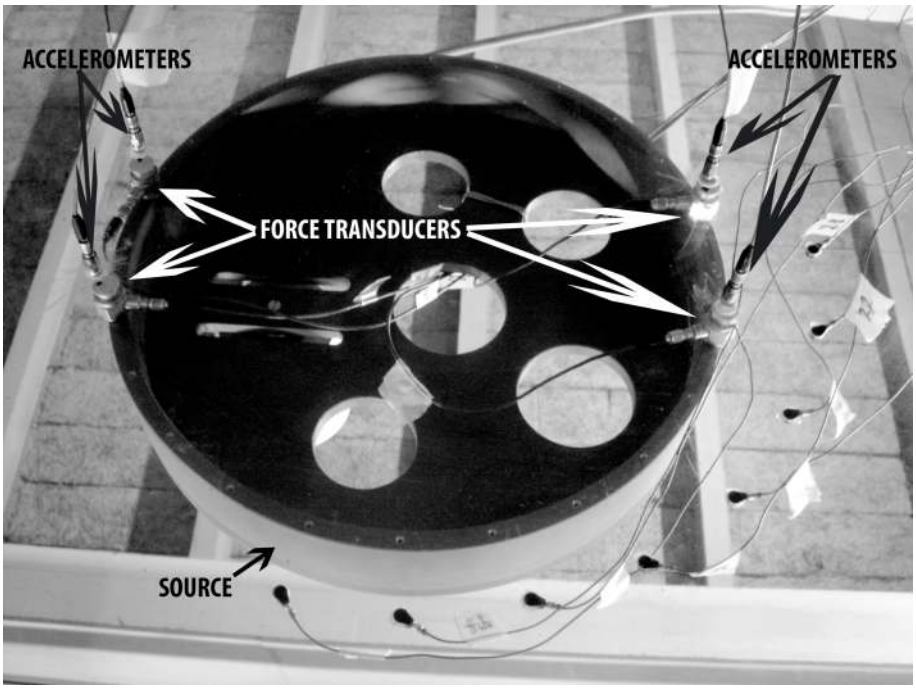


Figure 5: Experimental set up with the source (above the transparent plate), the force transducers (between the source and the plate) and the accelerometers (four of them mounted under the plate, in correspondence of the feet).

The plate has the following characteristics:

| | Symbol | Value |
|---|---|---|
| Length | L | 3050 mm |
| Width | W | 2050 mm |
| Thickness | h | 15 mm |
| Density | $\rho$ | 1150 kg/m$^3$ |
| Modulus of elasticity | E | $5.6 \cdot 10^9$ Pa |
| Poisson's ratio | $\mu$ | 0.37 ÷ 0.38 |

Table 1: The plate characteristics

The part of the plate available for the measurements is 1000 x 2000 mm, the remaining part of the edges is symmetrically embedded in sand.

### 3.1 Preliminary measurements

The developed theory provides good results only if it is applied to plates in which the reflections are not present. To check if the test rig corresponds to this task we can measure the point mobility and compare it with the infinite plate mobility whose expression is reported in equation (17). If the measured value is almost equal to the theoretical value, the plate can be treated as an infinite one. Another important preliminary data is provided by the coherence between the applied force and the measured velocity: a very high value is obtained after 60 Hz.
Exciting the plate with a random noise from 5 Hz up to 5 kHz the results shown in the following figures are obtained. Only the normalized mobility for one excitation point is plotted as the other show the same trend. It is possible to notice that the real part of this quantity is equal to one and the imaginary part is equal to zero in a wide frequency range.

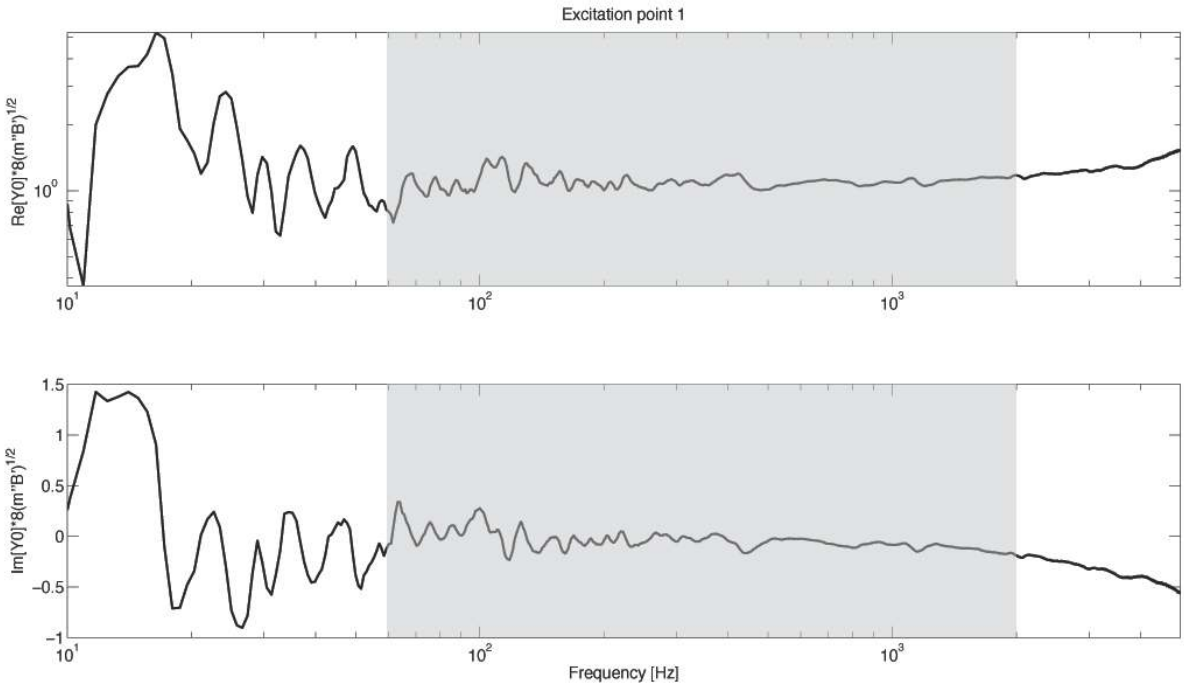


Figure 6: The real (upper plot) and the imaginary part (lower plot) of the normalized mobility.

At the end of the preliminary measurements it was clear that the reflections are negligible at least from 60, up to 2000 Hz (shaded area in Figure 6), so only in this frequency range the plate can be considered infinite. The mobility value at frequencies higher than 2000 Hz is different from the theoretical one because of the dimensions of the excitation point can be compared with the wavelength.

### 3.2 The inverse problem

To back-calculate velocity and force we need to know the velocity in the near field of the source. The velocity must be measured on two circles external to the four excitation point and, to avoid aliasing, it must be sampled $n_s$ times on each circumference. The formula to calculate $n_s$**,** based on the Nyquist criterion, is reported in equation (18).

$$n_s > \frac{4\pi r}{\lambda_{\min}}, \quad \lambda_{\min} = \left.\frac{2\pi}{k_b}\right|_{\min} \tag{18}$$

Where $r$ is the value of the radius of the circle used for measurements and $\lambda_{min}$ is the minimum value of the wavelength.
To establish the limit of validity of this theory, velocity has been measured on several external circles whose radiuses are reported in Table 2. The first three circles respect both the condition on the near field and on the number of sampling points in a wide frequency range, the fourth is a bit under sampled, and the last two are to far from the excitation points and under sampled. For these reasons we expect good results for the first two circular lines and worse results for the other. Since this prediction is respected, in Figure 7 is reported the comparison between the velocity measured in correspondence of the four excitation points (dash-dot line) and the velocity back–calculated (solid line) using the first two external circumferences. The frequency range studied has been previously determined in section 3.1.

| | Radius [mm] |
|---|---|
| Excitation points' circumference | 160 |
| 1st external circumference | 175 |
| 2nd external circumference | 190 |
| 3rd external circumference | 205 |
| 4th external circumference | 220 |
| 5th external circumference | 330 |
| 6th external circumference | 370 |

Table 2: Measurements' circumferences.

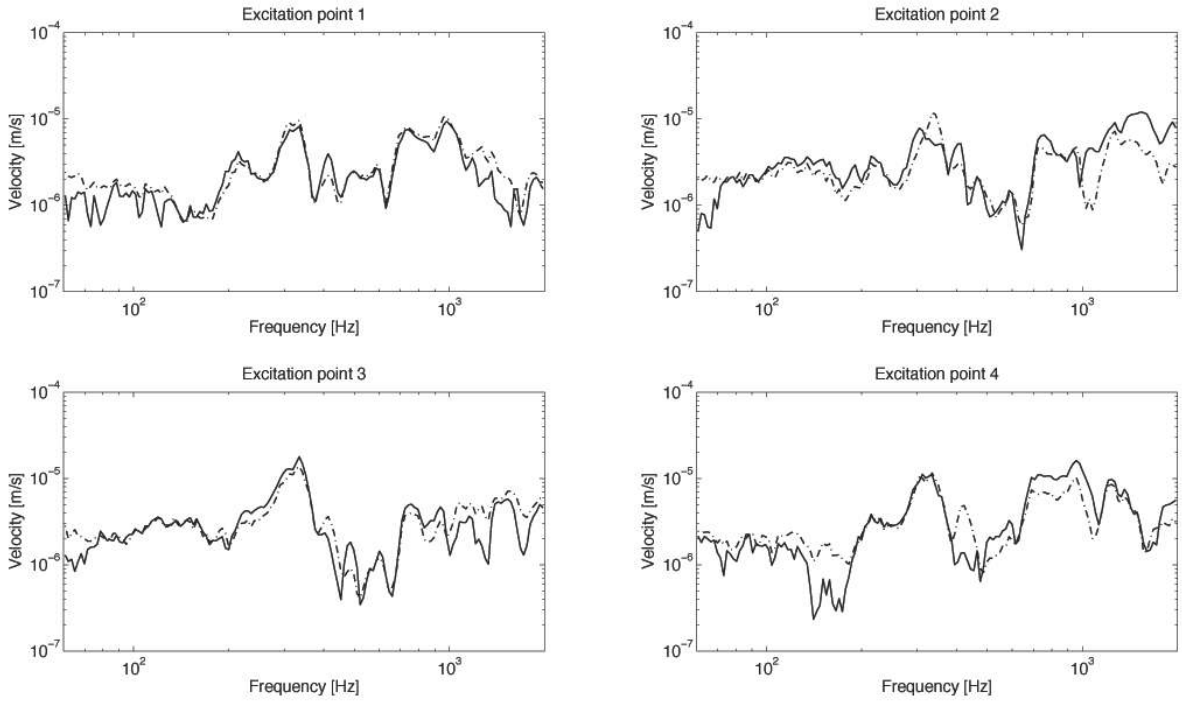


Figure 7: Comparison between the measured (dash-dot line) and the velocity back–calculated by using the measurements on the 1st and the 2nd circle (solid line).

Using the back-propagated velocity it is possible to back-calculate also the forces, as suggested in section 1.2. Of course, also in this case, the best result is obtained using as input data the velocity measured on the first two external circumferences. Results are shown in Figure 8.

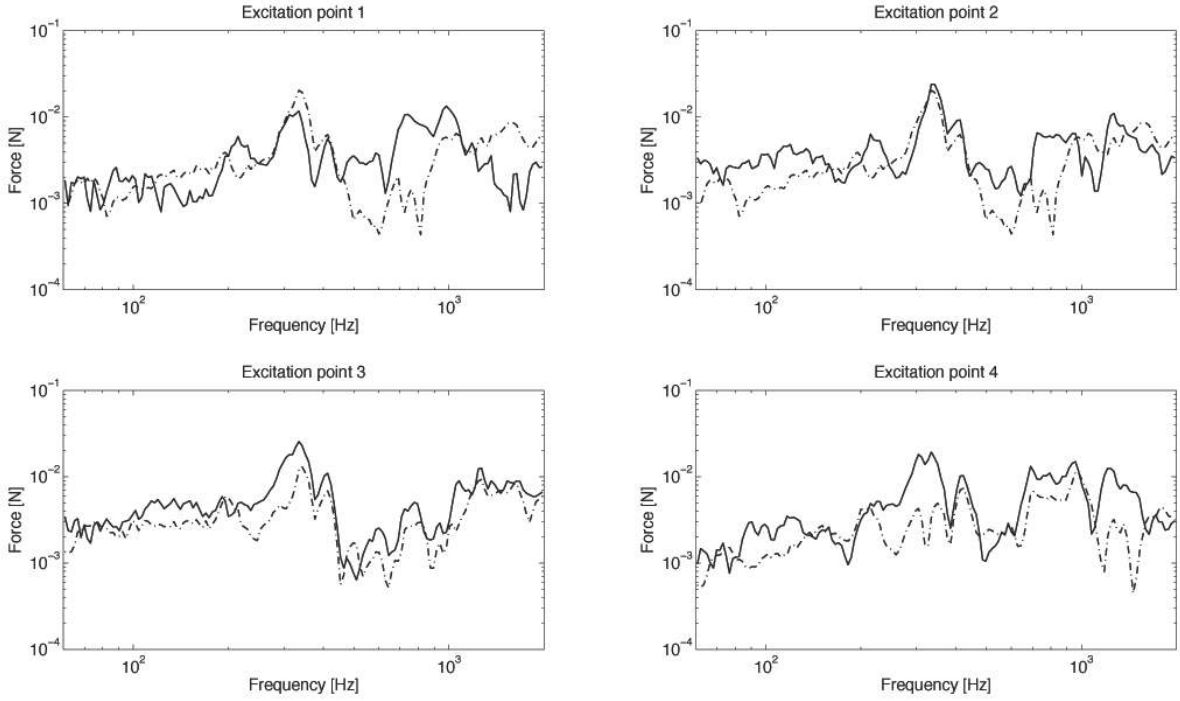


Figure 8: Comparison between the measured (dash-dot line) and the force back–calculated by using the measurements on the 1st and the 2nd circle (solid line).

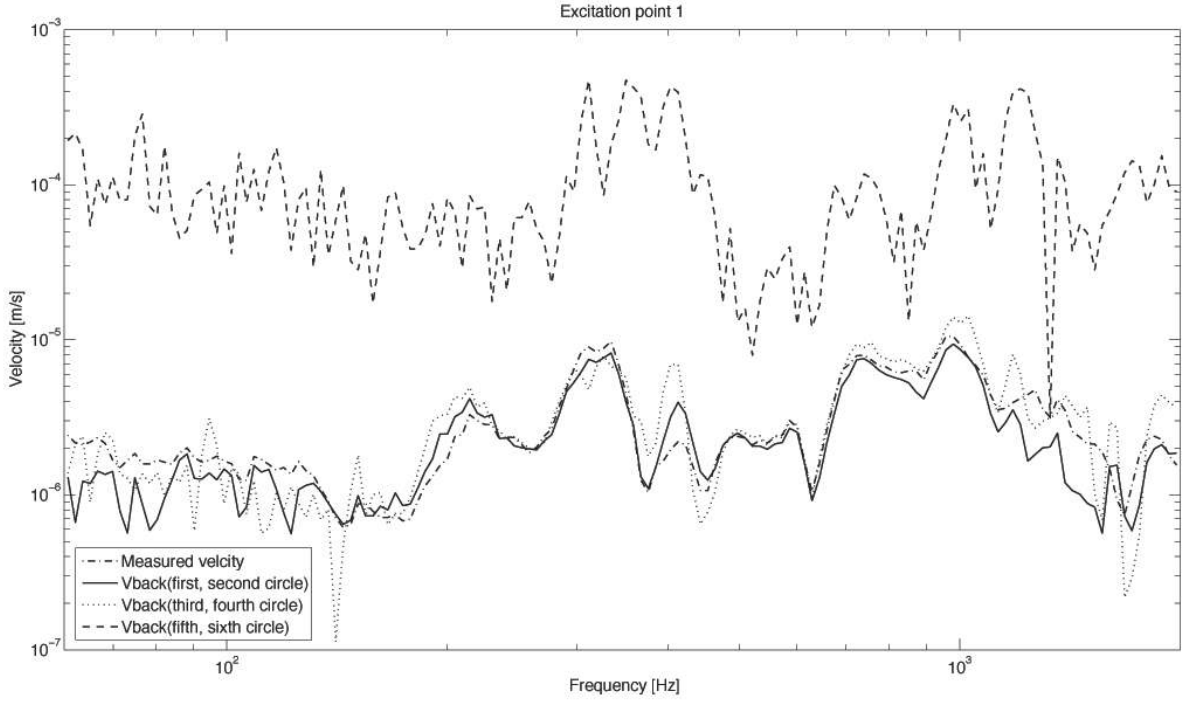


Figure 9: The back-calculated velocity by using circles in the near field and in the far field.

Once the velocity and the force at the interface are determined, the transmitted power can be calculated to fully characterize the source-receiver coupling.
The decrease in quality by using the other external circumferences has been investigated as well. Figure 9 depicts the comparison between the measured data (dash-dot line) and the velocity back-calculated by using circles both in the nearfield and in the far field. For sake of brevity the results for the other excitation points are omitted, as they show the same behaviour presented for the first excitation point. It is assumed that the near field is the region in which the relation given in equation (19) is satisfied [11]:

$$k_b d < 1 \tag{19}$$

Where $d$ is the distance between the excitation point and the external circle, measured along the radial coordinate. With reference to Table 2, only the first two circles are in the near field region for the whole frequency range. Nevertheless good results are obtained also using the measurements carried out along the third and the fourth circular line. Finally, for the infinite plate test case, we can state that the condition of equation (19) can be relaxed as stated in the following equation.

$$k_b d < 2 \tag{20}$$

## 4. CONCLUDING REMARKS

In the present work a theoretical platform for nearfield structure-borne sound holography has been developed. First of all, numerical simulations are undertaken to investigate the practicability of the theory and to study the applicability for an infinite plate excited by four point forces lying on a circular line. Then, an experimental test has been performed on a Perspex plate suitably designed to suppress the reflections from the boundaries.
To establish the validity limit of this procedure, a sensitivity analysis in terms of wavelength has been done. It is shown that the nearfield structure-borne sound holography provides good results for the infinite plate case in the first part of the far field too. The wavelength is also important in defining the proper number of points used to discretize the circular lines in the near field with respect to the Nyquist criterion. Since the quantities calculated using nearfield structure-borne sound holography show the same trends as the quantities directly measured on the plate, the results must be considered promising.
Nevertheless how nearfield structure-borne sound holography works with reflections remains to be analyzed. Eventually, nearfield structure-borne sound holography have to be assessed in semi-infinite plate, plate with discontinuities, plate with stiffeners, couplings with circular interfaces in order to obtain a useful tool for source characterization. In this sense the novel approach previously described could be helpful in calculating the field variables and the transmitted power for existing installations in which it is not possible to place a force transducer directly between the excitation source and the structure.

## ACKNOWLEDGEMENTS

The authors gratefully acknowledge the financial support received from the “European Doctorate in Sound and Vibration Studies” programme (EDSVS).

## REFERENCES

[1] S. E. S. Karlsson, Identification of External Structural Loads from Measured Harmonic Responses, Journal of Sound and Vibration, 196(1), 59-74, 1996.

[2] B. A. T. Petersson, B. M. Gibbs, Towards a Structure-Borne Sound Source Characterization, Applied Acoustics 61, 325-343, 2000.

[3] A. Tarantola, Inverse Problem Theory and Methods for Model Parameter Estimation, Society of Industrial and Applied Mathematics (SIAM), 2005.

[4] C. Pezerat, J. L. Guyader, Two Inverse Methods for Localization of External Sources Exciting a Beam, Acta Acustica 3, 1-10, (1995).

[5] C. Pezerat, J. L. Guyader, Identification of Vibration Sources, Applied Acoustics 61, 309-324, 2000.

[6] Y. Zhang, J. A. Mann III, Measuring the Structural Intensity and Force Distribution in Plates, Journal of the Acoustical Society of America 99, 345-353, 1996.

[7] Y. Zhang, J. A. Mann III, Examples of Using Structural Intensity and the Force Distribution to Study Vibrating Plates, Journal of the Acoustical Society of America 99, 354-361, 1996.

[8] E. G. Williams, Fourier Acoustics: Sound Radiation and Nearfield Acoustical Holography, Academic Press, London, 1999.

[9] A. W. Leissa, Vibrations of Plates, U. S. Government Printing Office, Washington, 1970.

[10] L. Cremer, M. Heckl, B. A. T. Petersson, Structure-Borne Sound, Structural Vibrations and Sound Radiation at Audio Frequencies, 3rd edition, Springer, Berlin, 2005.

[11] P. M. Morse, K. U. Ingard, Theoretical Acoustics, Princeton University Press, Princeton, 1986.